Scattering of Protons by Hydrogen Near 18 Mev*

J. L. YNTEMA† AND M. G. WHITE
Palmer Physical Laboratory, Princeton University, Princeton, New Jersey
(Received March 19, 1954)

The differential cross section for the scattering of 18.2±0.2-Mev protons by hydrogen has been measured over the angular range 30°–90° in the center-of-mass system. In order to reduce the over-all errors to less than 1 percent a 60-in. scattering chamber was used. Polyethylene, polystyrene, and nylon foils were used as scatterers while the proton-proton events were detected by observing coincidences between the scattered and recoil protons in anthracene photomultiplier counters. The incident proton beam was collimated to ±14 minutes of arc. Probable relative errors varied from 0.5 percent at 90° to about 1 percent at 30°, while the probable error in the absolute differential cross section at 90° is estimated to be 1 percent. The data show a significant deviation from pure S-wave scattering and are best fitted by taking S-, P-, and D-wave phase shifts to be $k_0=54.1°$, $k_1=+1.0°$, $k_2=+0.4°$, respectively.

I. INTRODUCTION

THE analysis of proton-proton scattering data obtained with incident proton energies of less than 10 Mev, using the method developed by Breit, Condon, and Present[1] has shown that in most cases these data are consistent with the assumption of only a S-wave phase shift. Breit and co-workers,[2] and Jackson and Blatt[3] have shown that, if one assumes that a central potential describes the interaction between protons adequately, the experimental data at these energies do not permit one to distinguish between different potential shapes. At higher energies one would expect to detect the presence of P- and D-wave phase shift, the magnitude of which would depend upon the assumed potential shape. Christian and Noyes[4] have shown that the data obtained by Panofsky and Fillmore,[5] and Cork, Johnston, and Richman[6] near 32 Mev do not show the expected P- and D-wave phase shift, but are consistent with the assumption of only a S-wave phase shift. Christian and Noyes have suggested the possibility of a masking of the P- and D-wave phase shifts, e.g., by a highly singular tensor interaction. If such a masking were present it might be less pronounced near 20 Mev than it would be at 30 Mev. However, the expected magnitude of the P- and D-wave phase shifts would be considerably smaller at 20 Mev than at 30 Mev and therefore harder to detect.

It was felt desirable to design the experiment so as to obtain a relative probable error of the order of one percent or less for the differential cross section between 30° and 90° in the center-of-mass system and to obtain an absolute probable error of one percent for the differential cross section at 90°.

II. DESIGN OF THE EXPERIMENT

The protons were supplied by the Princeton 35-in. synchrocyclotron. The available beam intensity after focusing by a magnetic lens system at 15 feet from the cyclotron was of the order of 10^{-9} amp over a 0.1-cm² area. The duty cycle of the cyclotron is about 2 to 5 percent depending upon the conditions of operation, with an average beam pulse length of about 15 microseconds. Hydrocarbon foils were used as target materials so as to obtain sufficient statistical accuracy in a reasonable time. The proton-proton events were detected by observing the coincidences between the scattered and recoil protons using anthracene crystals with photomultiplier tubes as detectors and a shorted line-type coincidence circuit.

The dimensions of the scattering chamber were determined by two requirements: (1) The solid angle subtended by the detector system was the one subtended by one of the apertures, which requires the solid angle subtended by the other, conjugate, aperture to be large enough to permit the entrance of all protons conjugate to the ones entering the defining aperture without introducing a prohibitively high single counting rate in either counter. (2) In determining the solid angle subtended by the defining counter one has to take into account the penetration of some protons through the edges of the aperture which causes the actual subtended aperture to be larger than the apparent one. In order for the effect to be negligible the area of the defining aperture should be large compared to the transparent area which sets a lower limit for the diameter of the aperture for a given permissible error. On the basis of these requirements a diameter of 60 in. was selected for the scattering chamber.

III. DESIGN OF THE 60-IN. SCATTERING CHAMBER

The scattering chamber, a vertical section of which is shown in Fig. 1, consists of a table B on which the target, defining apertures and detectors are mounted

* Supported in part by the U. S. Atomic Energy Commission and the Higgins Trust Fund.
† Present address: University of Pittsburgh, Pittsburgh, Pennsylvania.
[1] Breit, Condon, and Present, Phys. Rev. **50**, 825 (1936).
[2] G. Breit, Revs. Modern Phys. **21**, 238 (1951).
[3] J. Jackson and J. Blatt, Revs. Modern Phys. **22**, 77 (1950).
[4] R. S. Christian and H. P. Noyes, Phys. Rev. **79**, 85 (1950).
[5] W. K. H. Panofsky and F. L. Fillmore, Phys. Rev. **79**, 57 (1951); F. L. Fillmore, Phys. Rev. **83**, 1252(1951).
[6] Cork, Johnston, and Richman, Phys. Rev. **79**, 71 (1950).

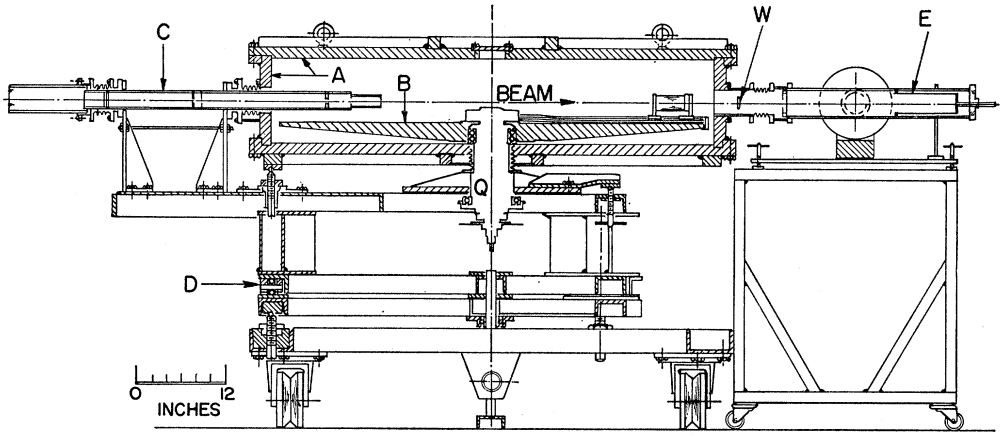

FIG. 1. The 60-inch scattering chamber. *A*, vacuum can; *B*, scattering table; *C*, beam collimating system; *D*, supporting structure; *E*, current collector; *Q*, table stem assembly; *W*, photographic plate holder.

and a collimation system *C*. It is necessary for the axis of the collimated beam to intersect with and be perpendicular to the axis of rotation of the chamber while the geometrical alignment obtained in air should not be affected by the evacuation of vacuum can *A*. This was achieved by having supporting structure *D* support both the collimation system *C* and, through table stem assembly *Q*, table *B*. The vacuum connection between *C* and *A* and *Q* and *A* are sylphon bellows which take up the deformation of *A* caused by evacuation without affecting the geometrical alignment obtained in air. Table stem assembly *Q* contained provisions for rotation of the table as well as for changing the angle between the two detectors while the system was evacuated.

1. Scattering Table *B*

The table was made out of aluminum 61ST6, its surface was machined flat to ± 0.005 in. and its thickness decreased from 2.75 in. at the center to 0.50 in. at the edge. Adjusting screws permit the table to be made accurately perpendicular to the axis of rotation of the table stem assembly *Q*. Care was taken to machine the central hole at the same time as the outer edge so as to insure concentricity. Graduation marks 0.012 in. wide were scratched in the outer edge every degree, or about 0.500 in. apart. Graduation accuracy was found to be better than two minutes of arc and by the use of a Bausch & Lomb microscope mounted outside the scattering chamber the angular position of the table could be located to better than 0.002 in.

2. Beam Collimation System

Adjustments for the beam collimation system are shown in more detail in Fig. 2. Collimating apertures 3 mm in diameter were mounted 75 cm apart inside a long, straight brass cylinder collimating the beam to ± 14 minutes of arc. Two lead baffle slits with 9-mm diameter apertures were used. One was located half-way in between the defining apertures and the other about 18 cm from the last aperture in a tube of smaller diameter so as to permit measurements to 172° in the laboratory system. The center line joining the two apertures must intersect and be perpendicular to the axis of rotation of the table with an accuracy greater than the spread in beam angle. This was achieved by the adjustments shown as follows. Translation in the horizontal plane is obtained through *A*, translation in the vertical plane through *B*. Rotation in the horizontal plane is obtained through *D* and in the vertical plane through *C* while spring *C'* presses the beam tube down on the top of screw *C*. After a satisfactory alignment has been obtained (perpendicular to the axis to better than 1 minute of arc and intersecting to ± 0.003 in.) the tube was clamped to the supporting brackets by rings as shown in Fig. 1. Sliding motion during evacuation was prevented by split-ring clamps around the tube.

3. Table Stem Assembly *Q*

The table stem assembly *Q* is shown in detail in Fig. 3. The main support for the table, 1, consists of a steel plate welded to a steel tube. This support was machined after the welding. The plate carries three arms which rest on the support structure through three tool steel, oil-hardened plates, one of which is flat, the second has a *V* groove and the third one a conical hole. The screws permit the leveling of support 1 and thus of the scattering table. The table has been bolted on to the steel ring which rests on a preloaded bearing. The tolerances on machining of these parts which locate the table position have been kept very small. The rotation of the table is made possible through Part 2. Part 3 is located with respect to Part 2 by a keyway and is press-fitted to the bearing. The vacuum seal between 1 and 2 is made through *V* rings as are the other vacuum seals in the table assembly. A worm gear system has been attached to Part 3. The latter can also be clamped so as to hold the table in place. Arm 5 is centered and rotated by a cylinder 4 which

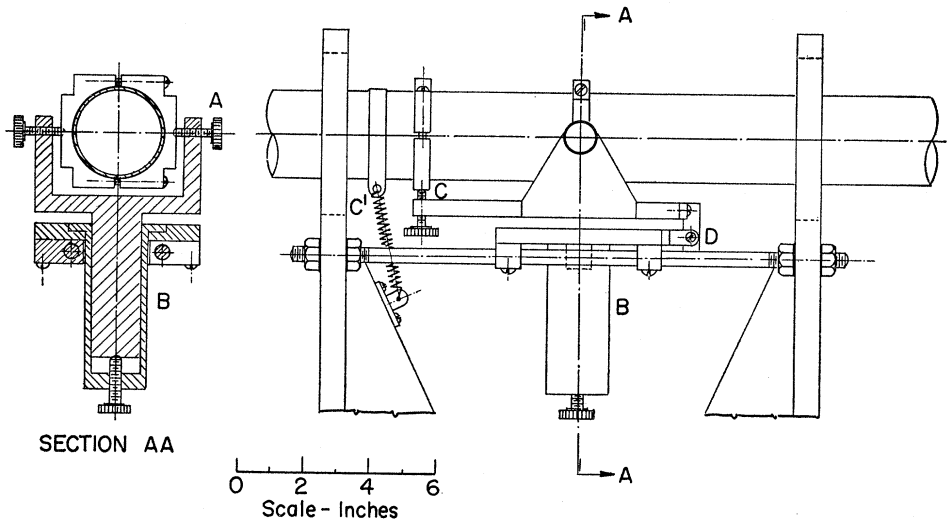

FIG. 2. Alignment of the collimating system. *A*, horizontal translation; *B*, vertical translation; *C*, *C'* rotation in vertical plane; *D*, rotation in horizontal plane.

also has a worm gear drive. Provisions were made to tie the motions of 2 to 4 by means of set screws. This required a clutch arrangement on the worm gear drive for arm 5. Arm 6 is centered by the upper bearing and is clamped to the edge of the table as shown.

The foil holder plate is carried by the top of the table stem assembly. Adjustments for lining up the axis of rotation in the plane of the foil have been provided for.

4. Supporting Structure

The motions required for aligning the scattering chamber with the deflected proton beam are translation, elevation, and leveling. The structure consists essentially of four frames. The bottom frame is made out of 6-in. ship channel. *V*-grooved swivel casters were bolted onto it. The vertical adjustment is made from this frame. A $\frac{1}{2}\times 20$ screw passes through a threaded block bolted to the channel. The height of the screw can be changed by turning a bolt which is supported by a ball bearing so as to eliminate unnecessary friction. A hardened steel ball rests on top of each screw and supports the second frame which has been made out of 4-in. ship channel. The balls rest against steel blocks, which have been bolted to the bottom of the second frame. On top of the channel, above the blocks, bearing plates have been mounted on which the third frame rests through ball bearings. These bearings are mounted in housings which have been bolted to columns welded to the top frame and are also bolted to the third frame. The two top frames thus form a unit which can rotate with respect to the two lower frames, over an angle of about 7°. This rotation is done by means of a screw with a fine thread. A bearing located under the second

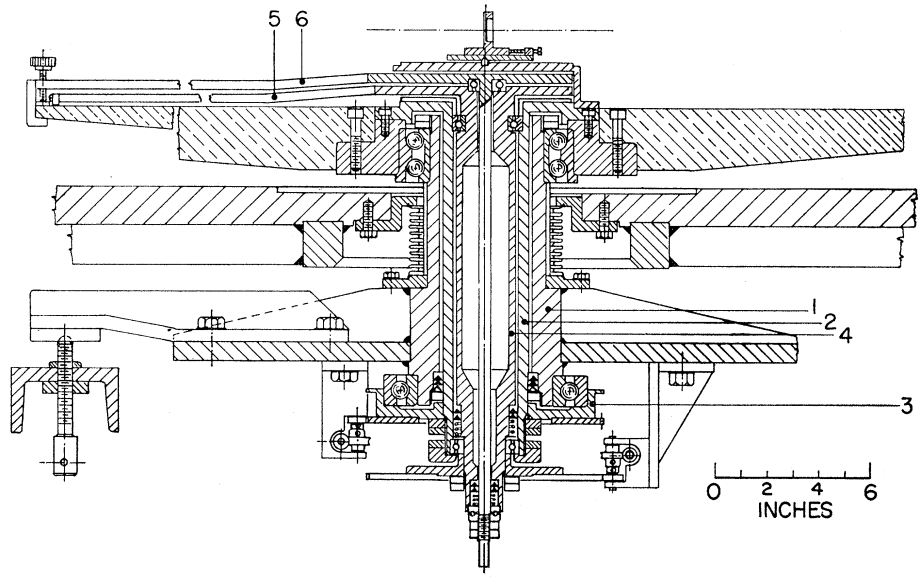

FIG. 3. Table stem assembly. *B*, scattering table; 1, table support; 5 and 6, arms for support of detectors.

frame keeps the two top frames from moving out. The top frame supports the beam collimating system and the scattering table. It also supports the vacuum can. The leveling of the vacuum can was accomplished through an arrangement similar to that used to level the structure with respect to the bottom frame.

5. Vacuum Can

The vacuum chamber consists of two reinforced steel plates and a cylinder. The cylinder is 12 in. high, $1\frac{7}{8}$ in. thick and has an interior diameter of 60 in. Top and bottom edges were machined down to a fine finish and two grooves for 0.210 O-rings were machined in. Two diametrically opposed holes serve as entrance and exit ports for the beam. A hole at 30° with the direction of the outgoing beam has been made to install a fixed angle monitoring counter. Two small holes for viewing the graduations at the edge of the scattering table were provided. The top and bottom plates are 1.5 in. thick; the top plate was reinforced with tack welded bars and the bottom plate with both bars and rings. The actual deflection measured with a dial indicator at the center of the bottom plate was 0.040 in. Holes have also been provided in the top and bottom plates for bringing in leads to the counters, for gas inlets, pressure gauges, and for the pumping unit.

IV. CURRENT INTEGRATOR

The collector cup is made of a heavy-wall 2.5-in. i.d. brass tube closed at one end by a heavy copper plate. On the inside the copper is covered with a sheet of graphite so as to reduce the fast neutron flux due to the stopping of 18-Mev protons. The cup is housed in a 4-in. o.d. brass tube, closed at the entrance by a 0.0015-in. Al foil which separates the vacuum inside the collector from that of the scattering chamber. At the back end the housing is closed by a polystyrene plate with a ground shield close to it. A 0.5-in. copper rod, screwed into the copper plate on the cup is brought out through an O-ring seal arrangement. The vacuum in the cup is generally held at 10^{-5} mm Hg. A magnet with 4-in. diameter pole tips is located as shown in Fig. 4. The magnetic field is approximately 300 gauss/amp in the normal region of operation. The current integration circuit is similar to the one constructed by Aamodt.[6] The copper rod is connected to a condenser and to an electrometer which is used as null indicating instrument. The collector cup is held very closely to ground potential through the compensating voltage supplied by batteries B through the intermediary of two 10-turn helipots of 500 and 150 ohms, respectively. The helipots are driven by a worm gear arrangement with a 1:60 reduction and operated by remote control. At the end of the run the voltage used to compensate for the charge due to the proton beam is measured on a Wolff-Feussner potentiometer, calibrated to 0.02 percent with a Leeds and Northrup Wenner potentiometer, through a 1:10 reduction provided by a volt box known to ±0.04 percent.

The capacitors were Unicon polystyrene capacitors ranging from 1.0 to 0.1 μf. They were calibrated by the National Bureau of Standards to ±0.2 percent using a time-constant current method. A recheck about one year after the original calibration of one of these capacitors showed a change of 0.5±0.2 percent in the originally reported value. The capacitors were calibrated at the temperature and relative humidity maintained during the experiment. The resistance was found to be of the order of 10^{14} ohms. Thus the time constants are of the order of 10^7 to 10^8 seconds. The upper limit for soakage in the dielectric was found to be 0.1 percent. Stray capacitances were found to have a negligible effect.

The electrometer used was a vibrating reed electrometer of the type described by Swank and Forstat.[7] With the input floating the resistance was of the order of 10^{16} ohm the input capacitance 10 μμf. The contact

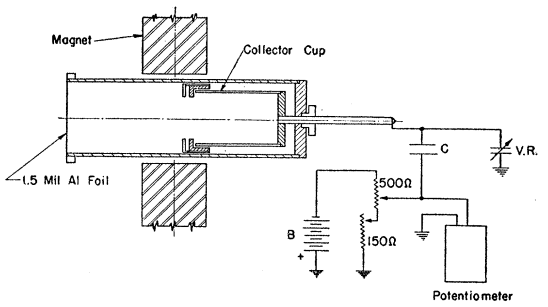

FIG. 4. Current integration circuit. C is calibrated condenser. $V.R.$ is vibrating reed electrometer. B is compensating voltage supply.

potential between reed and anvil was about 8 mv with a drift of less than 1 mv a day. The frequency of maximum converter efficiency was 292 cps. Since the instrument was used as null indicator only its absolute calibration was not important; usually it was operated at a sensitivity of about 5-mv full scale. This sensitivity permitted a fairly constant check on the current passing through the chamber.

It was felt desirable to make a certain number of checks on the consistency of the current integrator. In particular the integrated current should be independent of the voltage on the collector cup. Thin gold foils were used as targets and the detector was placed at an angle of about 7° with the outgoing beam. Since the cross section under those conditions varies to a good approximation with E_0^{-2}, where E_0 is the energy of the incident beam it was necessary to operate the cyclotron under constant conditions. The data given in Fig. 5 were obtained with a 0.0015-in. Al foil at the entrance and a field of approximately 500 gauss over the opening of the cup. The number of monitoring

[7] R. Swank and H. Forstat, Argonne National Laboratory Report CP3595 (unpublished).

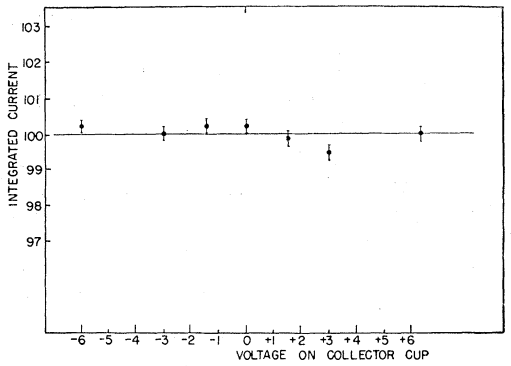

FIG. 5. Variation of integrated current as a function of voltage on the collector cup. The errors indicated are the standard deviation of the number of monitoring counts.

counts used was 300 000 and the error indicated is the standard deviation of the number of monitoring counts. In taking data the cup was always held within 0.5 v from ground potential.

The diameter of the cup was sufficient to collect all of the transmitted beam. This was checked by observing the diameter of the beam at W in Fig. 1 with spectroscopic plates. At this spot the beam diameter was always less than 10 percent of the diameter of the cup. It has been assumed that the transmitted beam is equal to the incident beam.

On the basis of the foregoing discussion it seems justifiable to assign an over-all error of ± 0.5 percent to the current integration circuit.

V. DETECTOR

The protons were detected by anthracene crystals in optical contact with RCA C7151 photomultiplier tubes. The pulses were clipped at the anode of the photomultiplier tube with a time constant of about 0.03 microsecond. Electrical breakdown around the photomultiplier tubes placed inside the vacuum can did not occur at pressures below 10^{-2} mm Hg.

The efficiency of the anthracene crystals has been checked by measuring the pulse height distribution of alpha particles from Po. It was assumed that the efficiency would be 100 percent for 5-Mev alpha particles. It was found that the average pulse height was about a factor 40 above the noise level. Varying the pressure in the system while keeping the geometry constant it was found that the probability for detecting 1.2-Mev alpha particles was 99 percent or higher. The effects of cracks in the crystal surface and other defects were investigated. These imperfections reduced the average pulse height by approximately 10 percent. Since the pulse height in anthracene at low energies is proportional to the range of the particle in the crystal and more or less independent of the nature of the particle, a 600-kev proton ought to be detected with more than 99 percent probability.

The protons scattered by hydrogen in the target are detected by observing the coincidences between the scattered and recoil protons. The problems of accidental coincidences and coincidence losses have been studied by Feather[8] and Westcott.[9] However it seems impractical to calculate the corrections and therefore the accidental coincidence rate was reduced as much as possible and the corrections were made experimentally. The coincidences were detected with a circuit similar to the one described by Bell, Graham, and Petch.[10] Since it was not possible to operate the photomultiplier tubes at very high voltages, the pulses were amplified by wide band amplifiers to produce the necessary pulse height for the cutoff of the tube.

The amplifiers which were used to amplify the pulses from the photomultiplier have been designed following Elmore's paper[11] and have a band pass of about 35 Mc/sec. The coincidence circuit had usually a resolving time of about 5×10^{-8} sec. The part of the pulse transmitted by the 1N34 diode in the case of a coincidence was amplified by a 25-Mc amplifier and from there fed in a scale of 16. The first stage of this scaler is identical to the one described by Fitch.[12] This stage will not trigger on pulses which are either much smaller or bigger than 5 volts. The fact that pulses smaller than 5 volts do not trigger this stage is used as a discriminator against the small pulses coming from the amplifier due to capacitive transmissions of single pulses by the biassed diode. Pulses bigger than 6 volts are limited by a diode circuit. The other stages of the scale of 16 are somewhat slower than the first stage but considerably faster than the usual design.

To count the number of accidental coincidences one changes the length of one of the cables from the cut-off tube to the shorted stub. If this length is increased by 15 meters coincidences due to proton-proton scattering are no longer recorded. The number of coincidences thus counted is taken to be the number of accidental coincidences.

The background can also be obtained if the included angle between the defining and conjugate counters is changed. In several cases this angle was changed from

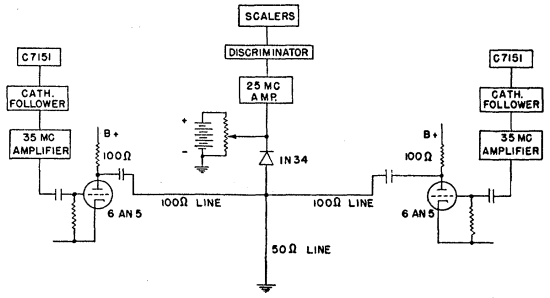

FIG. 6. Coincidence circuit.

[8] W. Feather, Proc. Cambridge Phil. Soc. **45**, 648 (1949).
[9] C. H. Westcott, Proc. Roy. Soc. (London) **A194**, 508 (1948).
[10] Bell, Graham, and Petch, Can. J. Phys. **30**, 35 (1952).
[11] W. C. Elmore, Nucleonics **5**, 48 (1949).
[12] Val Fitch, Rev. Sci. Instr. **20**, 942 (1950).

89.5° to about 86°. The results obtained were in substantial agreement with the delay line method, provided the beam intensity through the target was approximately the same. This may be taken to indicate that true coincidences, due to a $p,p\gamma$ reaction in carbon have a negligible effect.

The circuits were adjusted with a millimicrosecond pulse as described by Garwin.[13] This pulser was also used to check the behavior of the scale of 16. It was found that the first stage of this scaler will resolve two pulses separated by 0.07 μsec about 99 percent of the time.

When it was desirable to take single counting rates into any one channel the output of the cathode follower inside the vacuum can was connected directly to the input of a 25-Mc amplifier. The block diagram of the detection circuit is given in Fig. 6.

VI. DETERMINATION OF SOLID ANGLES

The solid angle subtended by the system is determined by the aperture of the defining counter and its distance from the center of the scattering. Circular apertures were used and their diameters measured both on a comparator and by direct comparison with a standard meter to about 1×10^{-3} mm. However, the effective diameter is different due to the slit edge penetration of the incident particles. It was felt desirable to estimate the effect of slit edge penetration experimentally. The number of particles which will be transmitted by the edges with an energy loss ΔE increases linearly with the diameter of the aperture while the solid angle subtended by the aperture increases with the square. Thus the relative effect decreases with r^{-1} if r is the radius of the aperture. Furthermore the effect, for small $\Delta E/E$, varies to a good approximation with E^2 where E is the energy of the particles incident on the aperture. Therefore the measurement of the cross section at, e.g., 25° and 65° with apertures with different radii ought to give an indication for the upper limit of the effect. If one compares runs 7 and 8 of Table II with runs 14 and 15 where the ratio of the aperture diameters was approximately 0.6 one can conclude that the effect is small. No corrections have been made for it in the final data.

The projected area of the defining aperture on the plane perpendicular to the radius vector from the scattering center will be fairly independent of the angle which the defining aperture makes with this plane, provided this angle be small. In general it has been possible to keep this angle smaller than 1° which gives an upper limit of error of 0.015 percent. The distance of the defining slit to the center of rotation of the scattering table was measured by two reading microscopes mounted on a rigid frame. The distance was measured by taking the difference between a standard length of 55.70 cm and the distance between the center and the aperture. This difference was of the order of a few millimeters and was measured with a traveling microscope. The target was placed at an angle of 45° with the scattered beam.

Since the solid angle subtended by the system was taken to be the solid angle $d\omega$ subtended by the defining aperture the angle subtended by the conjugate aperture $d\omega'$ has to be sufficiently large so as to admit all the protons conjugate to those entering the defining aperture. The geometrical relations are readily established. Another factor contributing to the spread of conjugate protons is the multiple scattering in the target. A reasonably good estimate for the required $d\omega'$ corresponding to a given $d\omega$ at an angle of scattering ϑ can be obtained. It was desirable, however, to ascertain experimentally that $d\omega'$ was large enough by measuring the cross sections for the different values of $d\omega'$ and increasing $d\omega'$ until the cross section remained constant. This could be done at all angles, except at the 30° point in the center-of-mass system. Though it appeared that the cross section remained constant and $d\omega'$ was larger than the calculated minimum value, it is felt that some uncertainty remains due to the limitations in the variation at this angle.

VII. TARGET MATERIAL

The target materials should be uniform over the area used, have negligible water absorption, accurately known chemical composition and be stable. These requirements seem to be met by polyethylene and polystyrene. The polyethylene was 0.0015 in. thick.[14] It has a very uniform gauge and no polymerizer is used in the polymerization. The polystyrene film used was 0.0005-in. cast polystyrene.[15] The water absorption was found to be less than 0.1 percent. A check on the presence of unpolymerized material was made and found to be less than 0.04 percent. No change in scattering cross section as a function of bombarding time was found. Both the polyethylene and polystyrene foils were analyzed by Mr. R. Paulsen of the National Bureau of Standards, Chemistry Division. The carbon and hydrogen content were determined by a semimacro method, using 0.5 to 0.8 gram per sample. The data are given in Table I, together with the estimated uncertainties.

The samples analyzed at the Bureau of Standards were considerably larger than the ones actually used in the experiments. The latter were about 1.00 in. $\times$1.75 in. and the polyethylene samples weighed about 36 mg each. However, since the composition is very well represented by CH_2 or CH as the case may be, there is little probability for a deviation from the chemical composition as determined by the semimacro method. The area of the foils used was measured to about 0.1 percent by direct comparison with the

[13] R. Garwin, Rev. Sci. Instr. **21**, 903 (1950).

[14] Obtained from E. I. Dupont de Nemours, Special Film Department.

[15] Obtained from Plax, Inc., Hartford, Connecticut.

TABLE I. Analysis of hydrocarbon foils.

Sample	%H	%C	Residue after combustion	%O
$(CH_2)^n$	14.38	85.59	0.03	0.08
	14.37	85.51	0.04	
	14.37	85.57	0.00	
$(CH)^n$	7.84	91.72	0.05	0.40
0.0005 in.	7.84	91.76	0.02	
$(CH)^n$	7.86	91.68	0.11	0.33
0.0008 in.	7.84	combustion	incomplete	
Estimated uncertainty	±0.02	±0.04		±0.02[a] ±0.04[b]

[a] For polyethylene.
[b] For polystyrene.

standard meter. The weight was determined to about 0.01 percent with a microbalance.[16] The uniformity of the polyethylene film was not measured directly. However, the cross sections obtained from three different foils and from different sections of the same foil are in excellent agreement and it is felt that a probable error of 0.4 percent describes the uniformity reliably. With polystyrene some idea of the uniformity may be obtained by observing green-light fringes in a Michelson interferometer. No high accuracy can be expected from such measurements. The data obtained with a 0.0005-in. polystyrene foil are in excellent agreement with the polyethylene data. In the measurements at 20°, 18°, and 15°, in the laboratory system it was desirable to use a somewhat thinner target. Targets of 0.0002-in. polyethylene[15] and 0.0005-in. nylon were used at these angles. Since the chemical composition of these foils was not known, the cross sections were calculated by comparison with respect to 25° or 30°.

VIII. ENERGY OF INCIDENT PROTONS

The energy of the incident beam was determined by a range measurement in Al of protons elastically scattered by carbon at 30°.[17] The protons were detected with a proportional counter 0.75 in. in diameter and filled at 32 cm with A and 2 percent of CO_2. The pulse-height discrimination was set so as to count only particles producing maximum ionization. The proportional counter was sealed with an Al foil of 7 mg/cm². The counter was placed 2 cm outside the scattering chamber. The peak of the distribution curve was found for a thickness of interposed Al of 458 mg/cm². The scattering foils used in these experiments were polyethylene films with a thickness of 0.00375 cm. The particles came out of the foil at a 30° angle and the mean loss of energy of the particles in the foil after scattering was estimated to be equivalent to 3 mg/cm² of Al. The protons thus have a total range of 472 mg/cm² in Al. If one uses the experimentally determined range of 18-Mev protons in Al[18] to correct the theoretically calculated range-energy curve one obtains a value for the energy of about 17.92 Mev. This corresponds to a value of 18.28 Mev for the energy of the incident protons, with an estimated error of ±0.2 Mev.

The proton beam is certainly not monoenergetic. However, since the cross section over the range 90° to 30° at this energy varies to a good approximation as E^{-1} some inhomogeneity will not affect the results. The results certainly would be affected by a variation in the mean value of the energy from run to run. There are indications that the mean value of the incident energy can be varied as much as 4 percent depending on the conditions of operation. However, since the value of the magnetic field was kept constant during the different runs and since the voltage on the deflector could not be varied much due to the strong collimation at the entrance of the chamber it is felt that the probable variation in mean energy is considerably smaller. Experiments in which gold was used as a scatterer and where the detector was placed at an angle where the cross section varies to a good approximation with E^{-2} indicated that the probable variation in E_0 was of the order of ±0.4 percent. One also has to consider the contribution to the cross section of a possible low-energy component in the beam. This component is mainly due to the collimating system of the scattering chamber. From calculations of Courant[19] it may be estimated that the apparent slit-widening effect is of the order of 0.5 percent. This estimate is based on the assumption that the detectors will not detect scattering due to particles with an energy of less than 75 percent of the mean energy of the incident beam. This assumption seems to be a reasonable one. The error due to this effect is negligible over the angular and energy range with which we are concerned in this experiment. There seems to be also a small low-energy tail at the exit of the cyclotron. This tail is, however, close enough to the mean value of the energy to be neglected.

IX. DATA

The cross sections have been calculated from

$$\sigma(\vartheta,E_0)=N\times 10^{24}/nId\omega.$$

The data are given in Table II. N is the total number of counts after a correction for accidental coincidences which never amounted to more than 2 percent and in most cases was about 0.3 percent. The observed voltage is proportional to the number of incident protons I. The number of hydrogen nuclei per cm² in the foil was obtained by the area-weight method. Since the target was always at a 45° angle to the scat-

[16] We are indebted to Dr. H. White of the Textile Research Institute, Princeton, New Jersey for his cooperation in the weighing of the samples.
[17] We are indebted to Mr. K. G. Standing for his help in this measurement.
[18] E. L. Hubbard and K. R. MacKensie, Phys. Rev. 85, 107 (1952).
[19] E. Courant, Rev. Sci. Instr. 22, 1003 (1952).

TABLE II. Summary of experimental data.

Run No.	Target	Angle lab. sys.	Angle c.m.	Counts	Voltage observed	$d\omega \times 10^5$	Reference value	Cross section millibarns/sterad
1	Polyethylene No. 3	45°	90°	40 900	3.4714	0.876		27.32
2	Polyethylene No. 3	45°	90°	41 000	3.4824	0.876		27.42
3	Polystyrene	45°	90°	40 890	10.3748	0.876		27.23
4	Polyethylene No. 4	45°	90°	15 070	1.1847	0.9465		27.33
5	Polyethylene No. 4	40°	80°	10 120	0.7329	0.9465		27.28
6	Polyethylene No. 4	35°	70°	15 130	1.0036	0.9465		27.53
7	Polyethylene No. 4	30°	60°	10 170	0.6269	0.9465		27.49
8	Polyethylene No. 4	25°	50°	10 130	0.5855	0.9465		27.25
9	Polyethylene No. 4	20°	40°	10 070	0.5436	0.9465		26.40
10	Polyethylene No. 4	45°	90°	45 996	1.3649	2.501		27.40
11	Polyethylene No. 4	40°	80°	61 256	1.6780	2.501		27.30
12	Polyethylene No. 4	35°	70°	29 850	0.7524	2.501		27.42
13	Polyethylene No. 4	55°	110°	46 000	1.6541	2.501		27.45
14	Polyethylene No. 4	60°	120°	30 520	1.2396	2.501		27.35
15	Polyethylene No. 4	65°	130°	14 975	0.7342	2.501		27.30
16	Polyethylene No. 7	45°	90°	20 460	1.6223	0.9465		27.12
17	0.2-mil Polyethylene	25°	50°	6 144	2.3087		27.27	
18	0.2-mil Polyethylene	20°	40°	6 116	2.1833			26.69
19	0.2-mil Polyethylene	18°	36°	6 120	2.1903			25.86
20	0.2-mil Polyethylene	15°	30°	10 025	3.5525			25.00
21	0.2-mil Polyethylene	18°	36°	6 055	2.1450			26.12
22	0.2-mil Polyethylene	25°	50°	7 130	2.6764		27.27	
23	Nylon	25°	50°	3 562	1.6498		27.27	
24	Nylon	15°	30°	3 040	1.3310			24.89

tered beam, this number has to be divided by $\cos(45° - \vartheta)$ to give the number n of hydrogen nuclei per cm^2 in the target. The data of runs 1 to 16 have been obtained from measured values of n, N, I, $d\omega$ and ϑ. Runs 17 to 22 and runs 23 and 24 give relative data. The cross sections at 20°, 18°, and 15° were obtained from the cross section at 25° which, from runs 8 and 15, was 27.27 mb/sterad.

The errors occurring in the measurement can be separated into two groups, those which affect the absolute measurement only and those which affect both the absolute and relative measurements.

1. Errors Which Affect Both the Relative and Absolute Values

(a) Statistics of counting. The standard deviation is the square root of the number of counts N taken. This standard deviation is slightly too low for those runs where the number of accidental coincidences was of the order of 1 to 2 percent.

(b) Fluctuation of incident energy. The fluctuation of energy as a function of time seems to be adequately represented by an error of 0.4 percent.

(c) The independence of the collected charge as a function of the voltage on the collector cup shows that fluctuations in the current integrator circuit do not introduce appreciable error.

(d) Penetration of the slit edges. Comparison of runs 7 and 8 with runs 14 and 15, respectively, shows that the contribution from this effect is small and can be neglected.

(e) The angle of the scatterer with the transmitted beam. This angle is introduced in the factor $\cos(45° - \vartheta)$. The maximum value for this angle is 30°. The uncertainty at this value is estimated to be less than 0.2° or 0.2 percent.

The estimated probable errors due to these effects varies from 0.5 percent at 90° to about 1 percent at 30°.

2. Errors Affecting the Absolute Values Only

(a) The area of the scattering foil was determined by direct comparison with a standard meter. The limit of error is estimated to be 0.15 percent.

(b) Weight of the scattering foil was measured with a microbalance with an error of less than 0.05 percent.

(c) The estimated error in hydrogen content was 0.2 percent.

(d) On the basis of runs 1, 2, 3, 4, 10, 16 of Table II the error due to lack of uniformity of the foils is estimated to be 0.4 percent.

(e) The diameters of the defining apertures were measured on two different comparators. The error is estimated to be 0.05 percent contributing an error of 0.1 percent in $d\omega$. The position of the slit as discussed previously introduces another error of $+0$, -0.015 percent.

(f) The distance of the slit to the center of the chamber is known ± 0.1 percent or better.

(g) ϑ is measured to about 2 minutes of arc. The error introduced is negligible in all points considered here.

TABLE III. Probable values and errors.

Angle	90°	80°	70°	60°	50°	40°	36°	30°
Probable value $(\text{mb/sterad})_{\text{c.m.}}$	27.32	27.29	27.47	27.42	27.27	26.50	25.98	25.00
Relative error	0.5%	0.5%	0.5%	0.6%	0.7%	0.8%	1%	1%

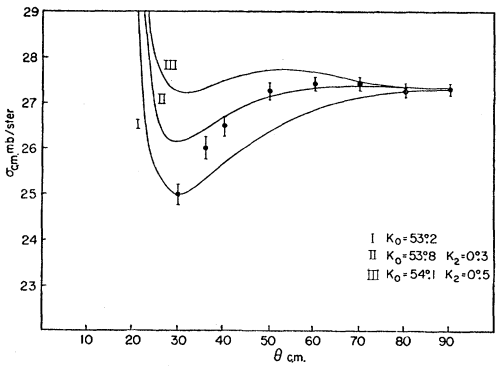

FIG. 7. Comparison of calculated distributions for various values of the S- and D-wave phase shifts with the experimental points. The S-wave phase shift was adjusted so as to give the experimental value for the cross section at 90°.

(h) Low energy component in the beam. On the basis of the discussion given above the error is estimated to be $+0$, -0.2 percent.

(i) The probable error in the current integration was estimated at ± 0.5 percent.

The combined rms error due to these effects is 0.8 percent and the estimated probable error in the cross section at 90° taking into account all errors is about 1 percent. The probable values of the cross section and the estimated probable errors are shown in Table III.

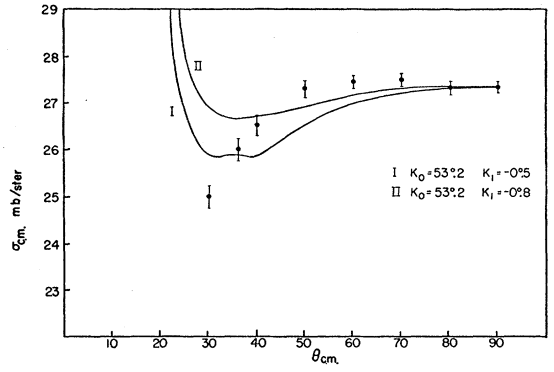

FIG. 8. Comparison of the calculated distribution for various combinations of S- and P-wave phase shifts. The S-wave phase shift was adjusted to give the experimental cross section at 90°.

X. THEORETICAL INTERPRETATION OF THE DATA

The theoretical distributions have been calculated using the formulas given by Breit, Condon, and Present.[1] The phase shifts were adjusted so as to give approximately the observed cross section at 90°. Figures 7, 8, and 9 give the distribution curves for the indicated values of the S-, P-, and D-wave phase shifts k_0, k_1, and k_2. Comparison of the distribution for an S-wave phase shift alone with the data, Fig. 7 curve I, shows that there is a deviation from S-wave scattering which we believe to be significant. It is seen that a combination of S- and D-wave phase shifts can give a reasonable agreement with the data if one assumes the observed 30° point to be about 3 or 4 percent low. Figure 8 shows that a combination of S- and P-wave phase shifts does not fit the data very well. If one adds an attractive P-wave phase shift to the $S+D$-wave distribution a very satisfactory fit may be obtained as shown in Fig. 9. If one uses the various values for the S-wave phase shift obtained by assuming 0°.0, 0°.3, and 0°.5 D-wave phase shifts one can calculate the f values which are found to be 23.7[4], 23.3[4], and 23.1[4]. These have been plotted in Fig. 10 on the curves of

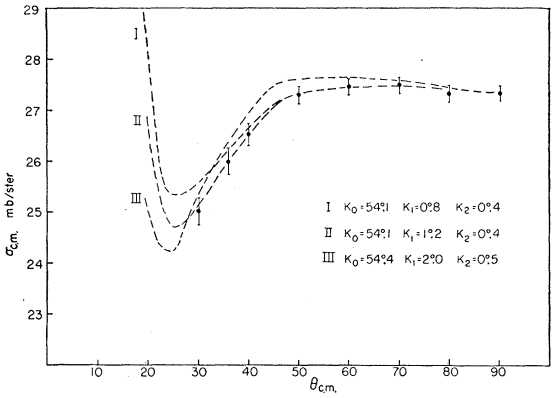

FIG. 9. Comparison of various combinations of S-, P- and D-wave phase shifts with the experimental values.

Yovits, Smith, Hull, Bengston, and Breit.[20] The estimated errors in the f values are ± 0.2. The value $k_0=53°.2$, obtained for $k_2=0$ has been included to permit comparison with f values obtained from data between 18 and 32 Mev by Cork,[21] where it was assumed that the cross section at 90° was due to S-wave scatter-

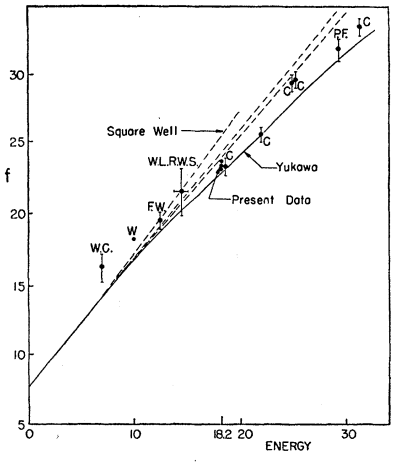

FIG. 10. Plot of the obtained values of the f function on the Fig. 1 of the paper by Yovits, Hull, Smith, Bengston, and Breit (see reference 20). The upper point corresponds to $K_0=53.2°$, the middle one to $K_0=53.8°$, and the lower one to $K_0=54.1°$. The error is about equal to the distance between two points.

[20] Yovits, Smith, Hull, Bengston, and Breit, Phys. Rev. **85**, 540 (1952).

[21] B. Cork, Phys. Rev. **80**, 321 (1950).

ing only. This shows that the S-wave scattering is of the magnitude expected from a Yukawa or exponential potential with the parameters fixed by the low-energy scattering. Figure 11 gives a comparison of the data with distribution curves to be expected from the potential proposed by Christian and Noyes.[22] It has been suggested that the discrepancy in the 90° values between the curves and the experimental point is not too important since a slight change in one of the available parameters could shift the curve vertically without any considerable change of shape. However, it is seen that the shape of the singlet square well plus triplet Yukawa tensor interactions is not satisfactory. The shape of the Gauss error potential plus triplet tensor interactions is satisfactory.

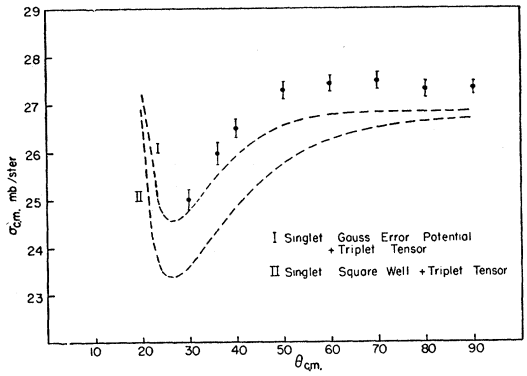

FIG. 11. Comparison of the experimental data with the potential proposed by Christian and Noyes (see reference 4).

ACKNOWLEDGMENTS

We are indebted to Dr. G. Breit for several very helpful discussions both on the experimental procedure and the interpretation of the data. The theoretical distribution curves given in Figs. 7, 8, and 9 were checked by Dr. M. H. Hull, Jr., Miss Smolen, Dr. Thaler, and Mr. Bengston. The assistance of Dr. J. C. D. Milton in the earlier stages of this work and of Mr. K. W. Brockman, Jr. in the taking of the data is gratefully acknowledged.

Most of the equipment was constructed in the shops of the Palmer Physical Laboratory. We are heavily indebted to the technical staff of the laboratory for their cooperation and many helpful suggestions.

[22] We are indebted to Dr. R. Christian for the calculation of the theoretical curves.

PHYSICAL REVIEW VOLUME 95, NUMBER 5 SEPTEMBER 1, 1954

Time-of-Flight Measurements on the Inelastic Scattering of 14.8-Mev Neutrons*

GERARD K. O'NEILL†
Laboratory of Nuclear Studies, Cornell University, Ithaca, New York
(Received May 25, 1954)

Measurements have been made of the energy spectra of neutrons inelastically scattered from 14.8 Mev into the interval 0.5–4 Mev. Carbon, aluminum, copper, tin, and lead scatterers were used. 100-kev deuterons were extracted from a cyclotron and allowed to strike a target of tritium absorbed in zirconium. The resulting reaction $T^3(d,n)He^4$ (17.7 Mev in the center-of-mass system) yielded a 14.8-Mev neutron accompanied by a recoil 3-Mev alpha particle. A scintillation counter within the vacuum system, subtending a solid angle of $4\pi/100$ at the target, detected recoil alpha particles with ~100 percent efficiency, delivering a fast signal whenever a neutron started on a path within a cone chosen to avoid scattering material for a distance of several meters. Within the cone and close to the target a scatterer was placed. The inelastically scattered neutrons emerged from the scatterer with approximate isotropy, while few elastically scattered neutrons were deflected through large angles. A proton-recoil neutron counter placed at ~90° to the cone axis was thus prevented from detecting almost all undesired neutrons. The distance from the scatterer to the counter was 50 to 100 centimeters, and neutron energies were obtained from the measured flight times over this path length, with the recoil alpha signal serving as a time zero. The flight times, which were from 20 to 65 millimicroseconds, were measured by a time analyzer having nine 4.7×10^{-9} second channels, recording directly on mechanical registers. Experimentally, neutron energies after scattering could be approximated by number/unit energy $E=E\exp(-E/T)$ with T, the "nuclear temperature" in Mev obtained from the raw data being: Pb, 0.75; Sn, 0.62; Cu, 0.84; Al, 1.06; C, 0.93. These results are in general agreement with photographic plate data. The experimentally observed angular distributions were isotropic within the limits of error of ~15 percent. Over-all limits of error of ±15 percent in the nuclear temperatures are assigned.

1. INTRODUCTION

IN studies of the internal structure of nuclei, measurements of inelastic neutron scattering (INS) are especially useful. Since neutrons do not interact with the Coulomb fields of nuclei or with atomic electrons, their scattering is a measure of nuclear properties alone and can be interpreted with few ambiguities.

In a complete inelastic scattering experiment, nuclei would be bombarded by monoenergetic neutrons, and the energy distributions of all subsequently emitted particles would be measured as functions of the angle from the incident neutron direction. For bombarding energies between 0.5 and 15 Mev, in all but the lightest

* Part of a Ph.D. thesis submitted to the faculty of the Graduate School of Cornell University. A preliminary report of this work was presented at the Spring, 1954, meeting of the American Physical Society, Phys. Rev. 95, 635(A) (1954).

† Present address: Physics Department, Princeton University, Princeton, New Jersey.